

## Boron and carbon: Antagonistic or complementary? Proposal for a simple prototype of a molecular clutch or molecular switch\*

Francesc Teixidor<sup>‡</sup> and Clara Viñas

*Institut de Ciència de Materials de Barcelona (CSIC). Campus U.A.B.,  
E-08193 Bellaterra, Spain*

**Abstract:** Boron and carbon, either in elemental form or when combined, are structurally very different. They are indeed complementary, and the weaknesses of one can be complemented by the strengths of the other, and vice versa. The structural complementarity can be readily observed in the shape of  $[X_nH_n]^{y-}$  ( $X = C$  or  $B$ ) compounds. One visualization of this complementarity can be found by comparing the most popular carbon and boron organometallic sandwich molecules,  $[Fe(C_5H_5)_2]$  and  $[3,3'-Co(1,2-C_2B_9H_{11})_2]^-$ . Both obey the  $18e^-$  rule, and in both the metal is  $\eta^5$  coordinated by two pentagonal faces. However, for  $[Fe(C_5H_5)_2]$ , the first ring of atoms outside the pentagonal face is coplanar with the coordinating face, whereas for  $[3,3'-Co(1,2-C_2B_9H_{11})_2]^-$  the substituents are out of the coordinating face featuring a canopy shading the metal. Taking advantage of this feature,  $[3,3'-Co(1,2-C_2B_9H_{11})_2]^-$  can be a well-performing molecular clutch electrochemically driven. When it is engaged, the beams of the upper  $[7,8-C_2B_9H_{11}]^{2-}$  ligand in  $[3,3'-Co(1,2-C_2B_9H_{11})_2]^-$  mesh the beams of the lower  $[7,8-C_2B_9H_{11}]^{2-}$ . This occurs when the molecular friction disk, the Co, is as  $Co^{3+}$ . When  $Co^{3+}$  is reduced to  $Co^{2+}$ , its radius is elongated, and both sets of beams are unmeshed allowing for a more free rotation, or molecular clutch disengagement.

**Keywords:** boron and carbon; carbon and boron; molecular clutches; molecular devices.

### COVALENT BORON AND CARBON

Boron is the neighbor element to carbon in the periodic table, both displaying the highest tendency to self-catenate. However, whereas carbon tends to have four connections when it self-catenates, boron tends to have more than four. In this regard, geometrical structures with triangular faces are commonly observed with boron hydrides. Noncombined boron exists in four major polymorphs:  $\alpha$ ,  $\beta$ ,  $\gamma$ , and T; in all of them the  $B_{12}$  icosahedron exists. This evidences the tendency of catenated boron atoms to fold to produce concave structures and contrasts with carbon. Therefore, getting the same structures in boron and carbon is highly unlikely. Carbon produces extended flat surfaces such as these found in graphite or in grapheme, which cannot be generated with boron. On the contrary, boron tends to produce compact polyhedral structures that cannot be made with carbon. Therefore, from the structural point of view boron and carbon are complementary, and this complementarity stretches beyond geometrical consid-

\**Pure Appl. Chem.* **84**, 2183–2498 (2012). A collection of invited papers based on presentations at the 14<sup>th</sup> International Meeting on Boron Chemistry (IMEBORON-XIV), Niagara Falls, Canada, 11–15 September 2011.

<sup>‡</sup>Corresponding author: E-mail: teixidor@icmab.es

erations as we shall show here. It is certain that quasi flat surfaces for  $B_{12}$  have been reasonably demonstrated [1] and that  $B_{80}$  has been predicted [2], but these are like small islands in an immense ocean.

The main practical difference between hydrocarbons ( $C_xH_y$ ) and boron hydrides ( $B_zH_w$ ) is that the first are naturally occurring, whereas the latter are artificial, and require energy to be made. This will always prevent the latter from competing in advantage to the first. However, boron hydrides can be valuable when their properties are not matched by apparently resembling organic molecules.

### $\pi$ -COMPLEXES

Most probably, cyclopentadienyl [ $C_5H_5$ ] $^-$ , Cp, is the more ubiquitous ligand in organometallic chemistry and ferrocene, see Fig. 1, reported in 1951 [3], the most derivatized organometallic framework [4]. Ferrocene is highly stable and undergoes many reactions characteristic of aromatic compounds, thus enabling the preparation of substituted derivatives. Ferrocene's ready reversibility at 0.64 V vs. SHE (standard hydrogen electrode) has paved its way to convert the molecule into one of the most widely utilized synthons in molecular materials in which an electrochemical response is sought. The geometrical main characteristic of ferrocene is the planarity of both cyclopentadienyl ligands, and the fact that they are parallel. As in any aromatic organic fragment, the C–H or C–R bonds in ferrocene beam out of the center of the aromatic fragment, therefore, substituents are largely coplanar with the aromatic ring. This facilitates rotation around the ferrocene axis, and the activation energy for rotation in ferrocene is low and similar to the one in ethane, 1–5 kcal mol $^{-1}$  [5]; the same is true for the isoelectronic cobaltocenium.

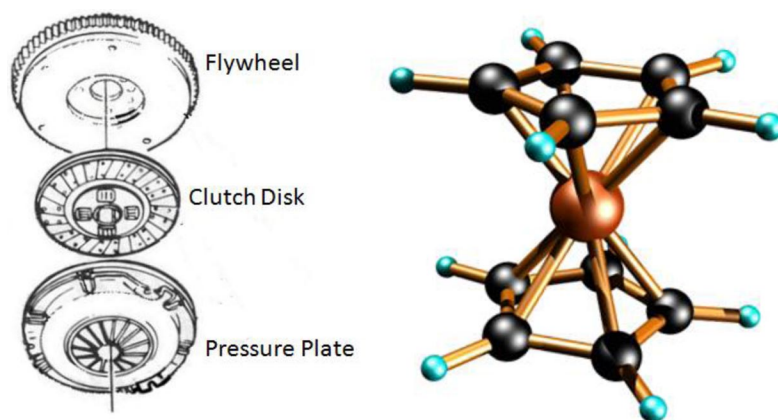


**Fig. 1** On the left, the components of a clutch are shown, whereas on the right the molecule of ferrocene is drawn. Both have three layers. The clutch disk in the ferrocene is the Co atom.

In 1965, a large set of metallabisdicarbollides with general formulae  $[3,3'\text{-M}(1,2\text{-C}_2\text{B}_9\text{H}_{11})_2]^{n-}$  ( $M = \text{Fe}, \text{Co}, \text{Ni}, \dots$ ) were reported [6]. Their shape can be viewed in Fig. 2E. In both ferrocene and metallabisdicarbollides, a feature to be highlighted is that the two pentagonal faces in each complex bind the metal in a  $\eta^5$  manner. Besides, in the same way as ferrocene (Fe(II)) obeyed the  $18e^-$  rule, many of the metallabisdicarbollides did. Examples that obey the  $18e^-$  rule are  $[3,3'\text{-Co}(1,2\text{-C}_2\text{B}_9\text{H}_{11})_2]^-$ ,  $[3,3'\text{-Fe}(1,2\text{-C}_2\text{B}_9\text{H}_{11})_2]^{2-}$ , and  $[3,3'\text{-Ni}(1,2\text{-C}_2\text{B}_9\text{H}_{11})_2]$ . However, the common way of finding the Fe, Co, and Ni metallabisdicarbollides is in a mononegative form, which implies that Co in the Co metallabisdicarbollide is  $\text{Co}^{3+}$  ( $d^6$ ), for Fe is  $\text{Fe}^{3+}$  ( $d^5$ ), and for Ni is  $\text{Ni}^{3+}$  ( $d^7$ ). Therefore, the one that in its natural appearance is a  $d^6$  is  $[3,3'\text{-Co}(1,2\text{-C}_2\text{B}_9\text{H}_{11})_2]^-$ , and with no doubt it has been the

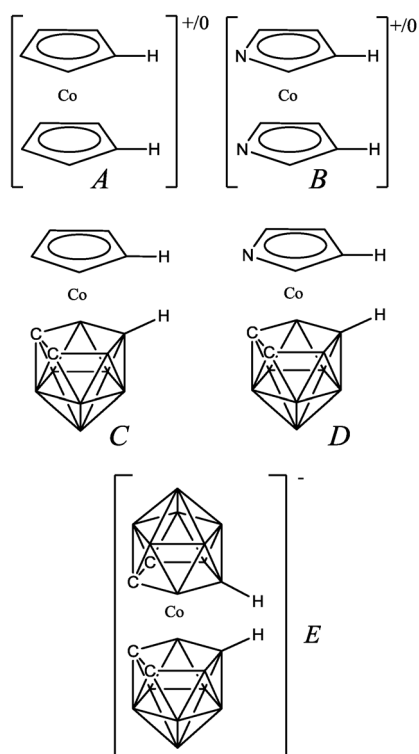


**Fig. 2** Representation of the sandwich complexes used in this work with Co as the metal ion, highlighting the H atoms of interest. The unspecified vertices in clusters correspond to B atoms.

one most studied [7], although when redox applications have been sought,  $[3,3'\text{-Ni}(1,2\text{-C}_2\text{B}_9\text{H}_{11})_2]^-$  has been preferred [8] due to its more attractive redox potential for the couple  $\text{Ni}^{4+}/\text{Ni}^{3+}$ .

Though famous and heavily investigated, ferrocene is nevertheless the only stable, metallocene sandwich of a first-row transition element; in contrast, carborane ligands form stable sandwiches with nearly all transition and lanthanide elements, as well as many main-group metals and metalloids [9]. Moreover, metallacarboranes in general can be reversibly oxidized and reduced to a far greater extent than can metallocenes. This enormously greater versatility of the metallacarboranes deserves greater acknowledgement than it generally receives.

### THE NONPLANARITY OF THE COORDINATING LIGAND'S FACE SUBSTITUENTS

A remarkable feature hardly recognized, if at all, is the pentagonal disposition of the ligand's substituents in  $[\text{C}_5\text{H}_5]^-$  and  $[7,8\text{-C}_2\text{B}_9\text{H}_{11}]^{2-}$ , when they are  $\eta^5$  coordinated to metal. In nonstrained ferrocene, these are coplanar with the ring (see Fig. 1), whereas in cobaltabisdicarbollide and any of the metallabisdicarbollides described before (see Fig. 5), the substituents are out of the coordinating plane featuring a canopy shading the metal. The off-plane angle has a value [10] near  $50 \pm 3^\circ$  that contrasts with an angle near  $0^\circ$  in ferrocene derivatives. This off-plane angle, which is responsible for the shadowing canopy around the metal, is a consequence of the globular nature of the borane ligand that forces the substituents to beam out the borane framework from its center through the cluster frame element. In the case of ferrocene, the substituents also beam out of the cyclopentadienyl framework, but because this is a plane, the substituent also remains in the plane. Therefore, had everything else been alike, the substituents on the metal binding pentagonal face already put a degree of discrepancy between  $[\text{C}_5\text{H}_5]^-$

and  $[7,8\text{-C}_2\text{B}_9\text{H}_{11}]^{2-}$ . Therefore, in what concerns the ease of rotation that is discussed in the following paragraphs, the  $[7,8\text{-C}_2\text{B}_9\text{H}_{11}]^{2-}$  should create a higher rotation barrier than  $[\text{C}_5\text{H}_5]^-$ , if everything else was constant.

## MOLECULAR CLUTCHES

Much has been discussed about molecular machines [11], but little about clutches although some proposed molecular machines perhaps could be better interpreted as molecular clutches [8]. A mechanical clutch, in its simplest application, is a device that has two rotating shafts passing power from one to another. See Fig. 1. The clutch connects the two shafts so that they may be locked together and spin at the same speed (engaged), locked together but spinning at different speeds (slipping), or unlocked and spinning at different speeds (disengaged). For the flywheel to motion the pressure plate, a friction clutch is required. When the clutch disk is worn, power from the flywheel is not transmitted to the pressure plate and the system that is in trouble, is equivalent to being disengaged. If there is no friction between the flywheel and the pressure plate, there is no transfer of motion from the driving to the driven member. The clutch task is to engage or disengage both shafts. How can this macroscopic behavior be converted into an equivalent one at the molecular level? As shown in Fig. 1, the resemblance between the macroscopic clutch and the sandwich ferrocene is notorious. The two cyclopentadienyl rings are equivalent to the flywheel and pressure plate and the Fe parallels the friction clutch. However, despite the similar physical appearance between the clutch device and ferrocene, the latter could not perform, as such, the task it was expected to do: engaging or disengaging the upper and lower parts of the device when it was required. The ease of rotation through the  $[\text{C}_5\text{H}_5]^-$  centroid(1)/Fe/ $[\text{C}_5\text{H}_5]^-$  centroid(2) axis, given by the low activation energy for the rotation of the  $[\text{C}_5\text{H}_5]^-$  rings, along with the impossible engagement/disengagement process does not allow ferrocene to be a good molecular clutch. This problem can be mitigated by impairing the free rotation through the axis by incorporating heteroatoms in the rings. This will produce a kind of electron pinning after incorporating electronic inhomogeneities in the aromatic ring. A modification of ferrocene that did incorporate a more electronegative atom (e.g., N) would accumulate electron density at this site and produce a localized *trans* effect that would raise the rotation activation energy. Very adequate examples would be  $[\text{Fe}(\text{NC}_4\text{H}_4)_2]$  or  $[\text{Co}(\text{NC}_4\text{H}_4)_2]^+$ , see Fig. 2B, however, none of them exists as such. Derivatives of the two, however, have been produced by blocking either all C positions with bulky groups or, alternatively, the two C positions nearest to N [12]. Probably, the existence of large substituents on the N-adjacent C atoms frustrates the  $\sigma$  donor capacity of N and the  $\eta^5$  pyrrolyl ligand is stabilized. The electronic pinning of N in diazaferrocene cannot be measured experimentally as, in substituted diazaferrocenes, it is altered by steric interactions. The first stable pristine  $\eta^5$  pyrrolyl complexes were reported in 1996 [13]. They needed to be mixed with a  $[7,8\text{-C}_2\text{B}_9\text{H}_{11}]^{2-}$  ligand. From this date, other examples were reported, all with the formulae  $[3\text{-Co}(\text{NC}_4\text{H}_4)(1\text{-R}_1\text{-2-R}_2\text{-1,2-C}_2\text{B}_9\text{H}_9)]$  ( $\text{R}_1 = \text{C}_6\text{H}_5, \text{C}_4\text{H}_9, \text{C}_3\text{H}_5, \text{CH}_3; \text{R}_2 = \text{H}$ ) [14–16] and ( $\text{R}_1 = \text{R}_2 = \text{CH}_3$ ) [17]. The C,C' propyl connected  $[3\text{-Co}(\text{NC}_4\text{H}_4)(1\text{-R-2-(CH}_2)_3\text{-1,2-C}_2\text{B}_9\text{H}_9)]$  ( $\text{R} = \text{CH}_3, \text{C}_6\text{H}_5$ ) was also produced [17]. In all of these, the substituents are only in the carborane moiety. The stability of these mixed  $\eta^5\text{-}[7,8\text{-C}_2\text{B}_9\text{H}_{11}]^{2-}/\eta^5\text{-}[\text{NC}_4\text{H}_4]^-$  compounds was fully proven by their ease of formation starting from N-derivatized pyrrole. Reaction of  $[\text{N}(\text{CH}_3)_4][7\text{-R-8-C}_4\text{H}_4\text{N-(CH}_2)_3\text{-7,8-C}_2\text{B}_9\text{H}_{10}]$  ( $\text{R} = \text{CH}_3, \text{C}_6\text{H}_5$ ) with  $\text{K}(\text{tBuO})$  and  $\text{CoCl}_2$  in dimethoxyethane leads to two complexes with the formulae  $[3\text{-Co}(\text{NC}_4\text{H}_4)(1\text{-R-2-C}_4\text{H}_9\text{-1,2-C}_2\text{B}_9\text{H}_9)]$  and  $[3\text{-Co}(\text{NC}_4\text{H}_4)(1\text{-R-2-C}_3\text{H}_5\text{-1,2-C}_2\text{B}_9\text{H}_9)]$  ( $\text{R} = \text{CH}_3, \text{C}_6\text{H}_5$ ) [14,18]. In both of them, a pristine pyrrole ligand has been generated from an N-substituted pyrrole. The  $2\text{-C}_4\text{H}_9$  and  $2\text{-C}_3\text{H}_5$  groups are produced from the cleavage of the spacer joining the pyrrolyl and carboranyl moieties in the original ligand. The  $[\text{N}(\text{CH}_3)_4]^+$  ion is necessary to produce the  $2\text{-C}_4\text{H}_9$  substituent [18]. The reaction is shown in Fig. 3. These results show the strong stabilizing power of  $[7,8\text{-C}_2\text{B}_9\text{H}_{11}]^{2-}$  that, contrarily to other  $\eta^5$  coordinating ligands such as  $[\text{C}_5\text{H}_5]^-$  or  $[\text{NC}_4\text{H}_4]^-$  anions has facilitated the first, and to date the only preparation of pristine  $\eta^5\text{-}[\text{NC}_4\text{H}_4]^-$  complexes. The

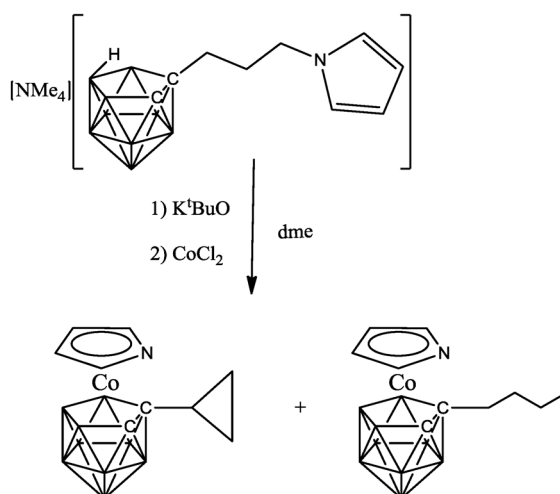


**Fig. 3** Evidence for the strong stabilizing power of  $[7,8\text{-C}_2\text{B}_9\text{H}_{11}]^{2-}$ .

crystal structures of all mixed cobaltacarboranes  $[3\text{-Co}(\text{NC}_4\text{H}_4)(1\text{-R}_1\text{-2-R}_2\text{-1,2-C}_2\text{B}_9\text{H}_9)]$  have the N projection on the  $\text{C}_2\text{B}_3$  plane bisecting the C–C bond.

The  $\text{N}_{\text{pyrrolyl}} \cdots \text{C}_{\text{cluster}}$  distance in  $[3\text{-Co}(\text{NC}_4\text{H}_4)(1,2\text{-C}_2\text{B}_9\text{H}_{11})]$  is 3.26(3) Å in RADCUU [13], comparable to the  $\text{C}_{\text{cp}} \cdots \text{C}_{\text{cluster}}$  in  $[3\text{-Co}(\text{C}_5\text{H}_5)(1,2\text{-C}_2\text{B}_9\text{H}_{11})]$ , 3.22(2) Å in DUBDIN01 [19a], or DUBDIN [19b]. The pinning of N in the  $[3\text{-Co}(\text{NC}_4\text{H}_4)(1\text{-R}_1\text{-2-R}_2\text{-1,2-C}_2\text{B}_9\text{H}_9)]$  complexes is already indicative of a preferential rotamer and consequently of a restricted rotation around the centroid(1)/M/centroid(2) axis. An energy profile for the rotation of  $[\text{NC}_4\text{H}_4]^-$  vs.  $[7,8\text{-C}_2\text{B}_9\text{H}_{11}]^{2-}$  in  $[3\text{-Co}(\text{NC}_4\text{H}_4)(1,2\text{-C}_2\text{B}_9\text{H}_{11})]$  is shown in Fig. 4.  $0^\circ$  corresponds to the N bisecting the  $\text{C}_{\text{cluster}}\text{-C}_{\text{cluster}}$  bond in  $[7,8\text{-C}_2\text{B}_9\text{H}_{11}]^{2-}$ . The activation energy is near  $9.5 \text{ kcal mol}^{-1}$  and is raised to near  $13 \text{ kcal}$

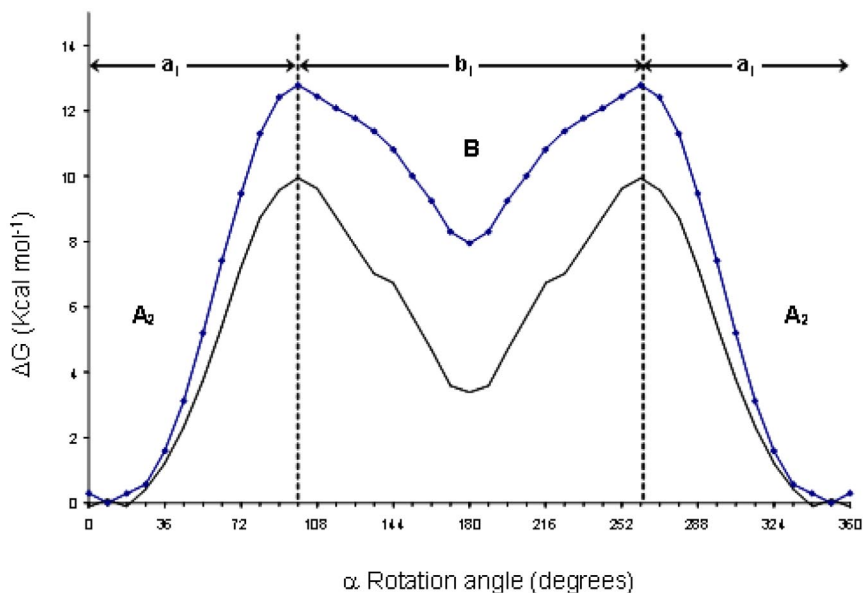


**Fig. 4** Energy profile for  $[3\text{-Co}(\text{NC}_4\text{H}_4)(7,8\text{-C}_2\text{B}_9\text{H}_{11})]$  (continuous line) and its adduct with  $\text{BF}_3$  (dotted line) calculated by the ZINDO/1 method [17].

mol<sup>-1</sup> when the adduct with BF<sub>3</sub> is generated. The engagement of [NC<sub>4</sub>H<sub>4</sub>]<sup>-</sup> with [7,8-C<sub>2</sub>B<sub>9</sub>H<sub>11</sub>]<sup>2-</sup> is stronger than the engagement of the two disks in ferrocene. The introduction of a heteroatom in the η<sup>5</sup> ligand has increased the friction between the two disks. However, the engaging/disengaging task expected in a clutch is not fully achieved.

## THE MOLECULAR CLUTCH

Five basic molecular structures will be addressed in which the central metal is common in all of them: cobaltocene, diazacobaltocene, mixed cyclopentadienyl/dicarbollide, and pyrrolyl/dicarbollide cobaltocene and cobaltabisdicarbollide complexes. The five frames are shown in Fig. 2. The current discussion will concentrate on the staggered H···H distance in these frameworks. This will be compared to the 2.40 Å that corresponds to the sum of two H Van der Waals (VdW) radii [20]. Staggered distances larger than the H···H VdW radii will be taken as indicative of nonfriction between the outer molecular disks. In [Co(C<sub>5</sub>H<sub>5</sub>)<sub>2</sub>], Co<sup>2+</sup>, DCYPCO04 [21], the H···H staggered distance is 3.495 Å. This distance shortens to 3.28 Å, (ACEXEL) [22] or 3.24 Å, (BIJRUI) [23] in [Co(C<sub>5</sub>H<sub>5</sub>)<sub>2</sub>]<sup>+</sup> (Co<sup>3+</sup>). Everything else being equal, the 0.21–0.25 Å shortening shall be assigned to the Co<sup>2+</sup> → Co<sup>3+</sup> contraction due to the higher oxidation state of Co, in [Co(C<sub>5</sub>H<sub>5</sub>)<sub>2</sub>]<sup>+</sup>. It results then, that in cobaltocenes in moving from Co<sup>3+</sup> → Co<sup>2+</sup>, an elongation occurs near 0.23 Å. In diazacobaltocene, whose pristine representation is on display in Fig. 2B, the staggered H···H distance would be near 3.143 Å as drawn from [Co(NC<sub>4</sub>(<sup>t</sup>Bu)<sub>2</sub>H<sub>2</sub>)<sup>+</sup> (Co<sup>3+</sup>), PIQNAE [24]. The H···H staggered distances are still too long compared to the H···H VdW radii to really represent a deterrent in the rotation through the centroid(1)/Co/centroid(2) axis. A noticeable H···H staggered distance shortening of the two rotating disks is achieved when the [7,8-C<sub>2</sub>B<sub>9</sub>H<sub>11</sub>]<sup>2-</sup> moiety is incorporated as one of the two outer disks in the molecular clutch. The main reference compound is [3-Co(C<sub>5</sub>H<sub>5</sub>)(1,2-C<sub>2</sub>B<sub>9</sub>H<sub>11</sub>)] (Co<sup>3+</sup>) [19a]. Two H···H distances are considered in these cases, the one due to C<sub>cluster</sub>-H···H<sub>Cp</sub> and the one due to B<sub>cluster</sub>-H···H<sub>Cp</sub>. The shorter distance should contribute more to the two outer disks friction. The B<sub>cluster</sub>-H···H<sub>Cp</sub>, 2.51 Å is shorter than the C<sub>cluster</sub>-H···H<sub>Cp</sub>, 2.749, see DUBDIN01 [19a]. The 2.51 Å H···H staggered distance is considerably shorter than with pure cobaltocenes, but still longer than the sum of two H VdW radii, 2.40 Å. A slightly longer H···H staggered distance is encountered when [C<sub>5</sub>H<sub>5</sub>]<sup>-</sup> is replaced by the pyrrolyl moiety [NC<sub>4</sub>H<sub>4</sub>]<sup>-</sup>, e.g., in [3-Co(NC<sub>4</sub>H<sub>4</sub>)(1,2-C<sub>2</sub>B<sub>9</sub>H<sub>11</sub>)] (Co<sup>3+</sup>) [13], in which the H···H distance is 2.61 Å.

The incorporation of [7,8-C<sub>2</sub>B<sub>9</sub>H<sub>11</sub>]<sup>2-</sup> has shortened the H···H staggered distance to levels very close to 2.40 Å, however, with only the pristine two outer disk molecules indicated above, it would not be sufficient to induce sufficient friction to deter rotation through the centroid(1)/Co/centroid(2) axis. Remarkably, [7,8-C<sub>2</sub>B<sub>9</sub>H<sub>11</sub>]<sup>2-</sup> has drawn nearer the two H atoms from the two distinct outer disks. By this perspective, the cobaltabisdicarbollide shown in Fig. 2E with two [7,8-C<sub>2</sub>B<sub>9</sub>H<sub>11</sub>]<sup>2-</sup> parts could provide attractive results on the H···H staggered distance. Indeed, this is the case, and distances in the range 2.20–2.40 Å have been encountered for [3,3'-Co(1,2-C<sub>2</sub>B<sub>9</sub>H<sub>11</sub>)<sub>2</sub>]<sup>-</sup> (Co<sup>3+</sup>) containing structures, e.g., DESZIL [25] ZAYOP [26], and CABZIQ [27] for B<sub>cluster</sub>-H···H-B<sub>cluster</sub>, B<sub>cluster</sub>-H···H-C<sub>cluster</sub> or C<sub>cluster</sub>-H···H-C<sub>cluster</sub>. Therefore, [7,8-C<sub>2</sub>B<sub>9</sub>H<sub>11</sub>]<sup>2-</sup> with Co<sup>3+</sup> provides a convenient clutch part to produce the molecular clutch sought. The H···H distance shortening to a value very close to the H···H VdW distance ensures a friction between the two constituent disks.

## ENGAGING AND DISENGAGING

The process of engaging and disengaging can be activated by switching on and off the inner molecular clutch disk. In the molecular clutch, the central clutch disk is a redox active metal. As described earlier, the Co<sup>3+</sup> → Co<sup>2+</sup> reduction expands the original Co<sup>3+</sup> diameter by near 0.23 Å, an amount sufficient to overcome the H···H VdW distance. This is possible if *d*, the distance between the eclipsed two H atoms,

is in the range  $2.40 \geq d \geq 2.17 \text{ \AA}$ . For  $[3,3'\text{-Co}(1,2\text{-C}_2\text{B}_9\text{H}_{11})_2]^-$  ( $\text{Co}^{3+}$ ), in which case the molecular clutch is engaged, the  $\text{H}\cdots\text{H}$  distance is near  $2.25 \text{ \AA}$ , therefore, upon reducing the central disk from  $\text{Co}^{3+} \rightarrow \text{Co}^{2+}$ , the  $d$  distance is expanded to near  $2.50 \text{ \AA}$ . This process is graphically depicted in Fig. 5 and quantitatively in Fig. 6.

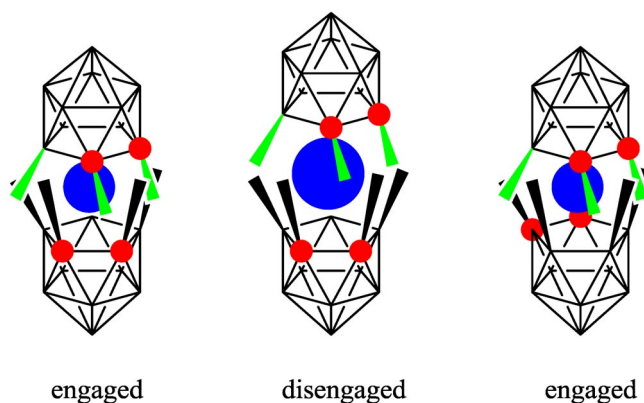


**Fig. 5** The engagement/disengagement process in  $[3,3'\text{-Co}(1,2\text{-C}_2\text{B}_9\text{H}_{11})_2]^-$ . The negative charge corresponding to each cluster has been omitted to emphasize the motif of interest.

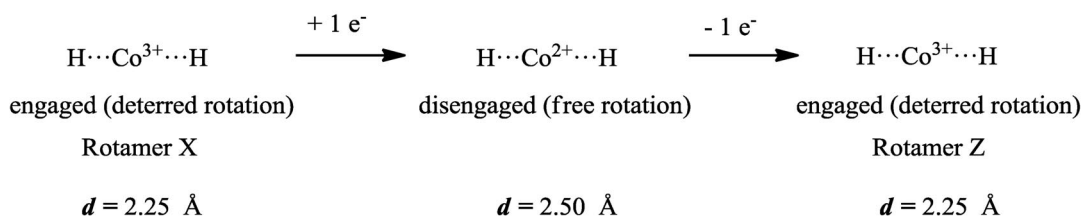


**Fig. 6** Expansion of Fig. 5. Rotamer X and Z are not necessarily the same.

It is noticeable the contrast between the in-plane H atoms of  $[\text{C}_5\text{H}_5]^-$  ligands and out-of-plane H atoms in the  $[7,8\text{-C}_2\text{B}_9\text{H}_{11}]^{2-}$  ligands. This is made even more interesting by the fact that in the pentagonal-pyramidal  $[2,3\text{-R}_2\text{-}2,3\text{-C}_2\text{B}_4\text{H}_4]^{2-}$  ligands the basal H atoms are directed away from the metal in  $[3,3'\text{-M}(1,2\text{-C}_2\text{B}_4\text{H}_6)_2]^{x-}$  ( $\text{M} = \text{Co}$ ,  $x = 1$ ;  $\text{M} = \text{Fe}$ ,  $x = 2$ ) sandwich complexes [28]. The crystal structures of  $[3,3'\text{-Co}(1,2\text{-C}_2\text{B}_9\text{H}_{11})_2]^-$  (CABZIQ) [27] and  $[1\text{-Co}(2,3\text{-(C}_2\text{H}_5)_2\text{-}2,3\text{-C}_2\text{B}_4\text{H}_4)_2]^-$  (WAVPEO) [29] displaying the H atoms are shown in Fig. 7. Of relevance is the dissimilar arrangement of the H atoms in the  $\eta^5\text{-C}_2\text{B}_3$  coordinating planes of  $[7,8\text{-C}_2\text{B}_9\text{H}_{11}]^{2-}$  and  $[2,3\text{-R}_2\text{-}2,3\text{-C}_2\text{B}_4\text{H}_4]^{2-}$  ligands. This arrangement in  $[2,3\text{-R}_2\text{-}2,3\text{-C}_2\text{B}_4\text{H}_4]^{2-}$  ligands prevents “gear-meshing” contrarily to what occurs in the  $[3,3'\text{-Co}(1,2\text{-C}_2\text{B}_9\text{H}_{11})_2]^-$  dicarbollide complexes discussed here, but it allows facile oxidative fusion of the ligands to form neutral  $\text{R}_4\text{C}_4\text{B}_8\text{H}_8$  cages with ejection of the metal, something not seen in the dicarbollide complexes [30].

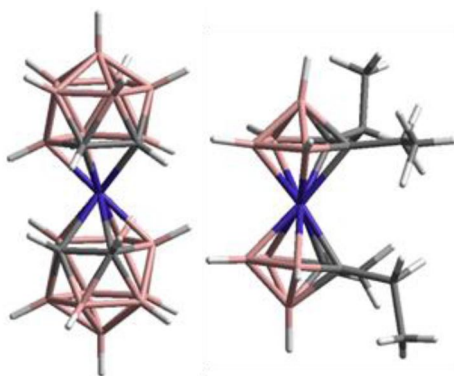


**Fig. 7** Crystal structures of  $[3,3'\text{-Co}(1,2\text{-C}_2\text{B}_9\text{H}_{11})_2]^-$  (CABZIQ) [26] and  $[1\text{-Co}(2,3\text{-(C}_2\text{H}_5)_2\text{-}2,3\text{-C}_2\text{B}_4\text{H}_4)_2]^-$  (WAVPEO) [31] displaying the H atoms. Of relevance is the dissimilar arrangement of the H atoms in the  $\text{C}_2\text{B}_3$  planes. In  $[3,3'\text{-Co}(1,2\text{-C}_2\text{B}_9\text{H}_{11})_2]^-$  the H atoms tend to protect the Co, whereas in  $[1\text{-Co}(2,3\text{-(C}_2\text{H}_5)_2\text{-}2,3\text{-C}_2\text{B}_4\text{H}_4)_2]^-$  the H atoms tend to avoid the metal.

## CONCLUSIONS

Conceptually, the most popular carbon and boron organometallic sandwich molecules,  $[\text{Fe}(\text{C}_5\text{H}_5)_2]$  and  $[3,3'\text{-Co}(1,2\text{-C}_2\text{B}_9\text{H}_{11})_2]^-$ , are very comparable. They are geometrically very similar: (i) both have the metal  $\eta^5$  coordinated with planar pentagonal faces, (ii) are  $18e^-$  organometallic compounds, and (iii) are electroactive species. However, they show a marked discrepancy in what refers to the angles of the bond H–C in  $[\text{C}_5\text{H}_5]^-$  and B–H/C–H in  $[7,8\text{-C}_2\text{B}_9\text{H}_{11}]^{2-}$  with regard to the plane of the corresponding  $\eta^5$  coordinating face. Whereas, for H–C ( $[\text{C}_5\text{H}_5]^-$ ) the angle is near to  $0^\circ$  it is near  $50^\circ$  for  $[7,8\text{-C}_2\text{B}_9\text{H}_{11}]^{2-}$ . This implies that in the latter, the B–H bonds in one  $[7,8\text{-C}_2\text{B}_9\text{H}_{11}]^{2-}$  mesh the B–H bonds in the second  $[7,8\text{-C}_2\text{B}_9\text{H}_{11}]^{2-}$ , resulting in a hindered relative rotation of both dicarbollide units. This does not occur with  $[\text{Fe}(\text{C}_5\text{H}_5)_2]$ , which can freely rotate one  $[\text{C}_5\text{H}_5]^-$  with regard to the second. The meshing of the B–H bond in one  $[7,8\text{-C}_2\text{B}_9\text{H}_{11}]^{2-}$  is just sufficient to restrict rotation, however, upon reduction of the central atom from  $\text{Co}^{3+} \rightarrow \text{Co}^{2+}$ , an elongation occurs producing a separation of the two  $[7,8\text{-C}_2\text{B}_9\text{H}_{11}]^{2-}$  units that unrestrict the rotation. This system  $[7,8\text{-C}_2\text{B}_9\text{H}_{11}]^{2-}/\text{Co}/[7,8\text{-C}_2\text{B}_9\text{H}_{11}]^{2-}$  therefore permits engagement/disengagement/engagement of the two  $[7,8\text{-C}_2\text{B}_9\text{H}_{11}]^{2-}$  units becoming a molecular clutch. As a consequence, we propose  $[3,3'\text{-Co}(1,2\text{-C}_2\text{B}_9\text{H}_{11})_2]^-$  and for extension also with Fe,  $[3,3'\text{-Fe}(1,2\text{-C}_2\text{B}_9\text{H}_{11})_2]^-$ , as a first model of a molecular clutch that can be electrochemically driven and that can be a key component of molecular machines.

## REFERENCES AND NOTES

1. H. J. Zhai, B. Kiran, J. Li, L. S. Wang. *Nat. Mater.* **2**, 827 (2003).
2. N. G. Szwacki, A. Sadrzadeh, B. I. Yakobson. *Phys. Rev. Lett.* **98**, 166804 (2007).
3. T. J. Kealy, P. L. Pauson. *Nature* **168**, 1039 (1951).
4. P. Stepnicka (Ed.). *Ferrocenes: Ligands, Materials and Biomolecules*, Wiley-Blackwell (2008).
5. (a) L. N. Mulay, A. Attalla, *J. Am. Chem. Soc.* **85**, 702 (1963); (b) S. Sorriso, G. Cardaci, S. M. Murgia. *J. Organomet. Chem.* **44**, 181 (1972).
6. M. F. Hawthorne, D. C. Young, P. A. Wegner. *J. Am. Chem. Soc.* **87**, 1818 (1965).
7. I. B. Sivaev, V. I. Bregadze. *Collect. Czech. Chem. Commun.* **64**, 783 (1999).



8. (a) M. F. Hawthorne, J. I. Zink, J. M. Skelton, M. J. Bayer, C. Liu, E. Livshits, R. Baer, D. Neuhauser. *Science* **303**, 1849 (2004); (b) A. M. Spokoyny, T. C. Tina, O. K. Farha, C. W. Machan, C. She, C. L. Stern, T. J. Marks, J. T. Hupp, C. A. Mirkin. *Angew. Chem., Int. Ed.* **49**, 5339 (2010).
9. R. N. Grimes. *Carboranes*, 2<sup>nd</sup> ed., Elsevier, New York (2011).
10. The angle has been computed after studying several crystal structures incorporating the anion  $[\text{Co}(\text{C}_2\text{B}_9\text{H}_{11})_2]^-$  found in the Cambridge Structural Database (CSD).
11. (a) T. Ross Kelly (Ed.). *Molecular Machines* (Topics in Current Chemistry), Springer (2006); (b) J. F. Stoddart *Acc. Chem. Res.* **34**, 410 (2001); (c) B. Roux (Ed.). *Molecular Machines*, World Scientific Publishing (2011).
12. (a) N. Kuhn, E. M. Horn, R. Boese, N. Augart. *Angew. Chem., Int. Ed. Engl.* **27**, 1368 (1988); (b) N. Kuhn, M. Kockerling, S. Stubenrauch, D. Blaser, R. Boese. *J. Chem. Soc., Chem. Commun.* 1368 (1991); (c) N. Kuhn, S. Stubenrauch, D. Blaser, R. Boese. *Z. Naturforsch., B: Chem. Sci.* **54**, 424 (1999).
13. M. Lamrani, S. Gomez, C. Vinas, F. Teixidor, R. Sillanpaa, R. Kivekas. *New J. Chem.* **20**, 909 (1996).
14. F. Teixidor, S. Gomez, M. Lamrani, C. Vinas, R. Sillanpaa, R. Kivekas. *Organometallics* **16**, 1278 (1997).
15. J. Llop, C. Vinas, F. Teixidor, L. Victori, R. Kivekas, R. Sillanpaa. *Organometallics* **20**, 4024 (2001).
16. J. Llop, C. Vinas, F. Teixidor, L. Victori, R. Kivekas, R. Sillanpaa. *Organometallics* **21**, 355 (2002).
17. C. Vinas, J. Llop, F. Teixidor, R. Kivekas, R. Sillanpaa. *Chem.—Eur. J.* **11**, 1933 (2005).
18. S. Gomez, C. Vinas, M. Lamrani, F. Teixidor, R. Kivekas, R. Sillanpaa. *Inorg. Chem.* **36**, 3565 (1997).
19. (a) J. G. Planas, C. Viñas, F. Teixidor, M. E. Light, M. B. Hursthouse. *CrystEngComm* **9**, 888 (2007); (b) P. E. Smith, A. J. Welch. *Organometallics* **5**, 760 (1986). The values for DUBDIN01 have been taken in preference to these for DUBDIN due to a lesser discrepancy of the distinct C–H···H–B distances, most probably due to a lower R value.
20. A. Bondi. *J. Phys. Chem.* **68**, 441 (1964).
21. M. Y. Antipin, R. Boese, N. Augart, G. Schmid. *Struct. Chem* **4**, 91 (1993).
22. F. A. Cotton, L. M. Daniels, C. C. Wilkinson. *Acta Crystallogr., Sect. E: Struct. Rep.* **57**, m529 (2001).
23. J. M. Migliori, W. M. Reiff, A. M. Arif, J. S. Miller. *Inorg. Chem* **43**, 6875 (2004).
24. N. Kuhn, R. Fawzi, H. Kotowski, H. Steinann. *Z. Kristallogr., New Cryst. Struct.* **212**, 437 (1997).
25. E. V. Mutseneck, Z. A. Starikova, K. A. Lyssenko, P. V. Petrovskii, P. Zanello, M. Corsini, A. R. Kudinov. *Eur. J. Inorg. Chem.* **14**, 4519 (2006).
26. T. M. Polyanskaya, V. V. Volkov, M. K. Drozdova. *Zh. Strukt. Khim.* **44**, 632 (2003).
27. E. J. Juarez-Perez, R. Nunez, C. Vinas, R. Sillanpaa, F. Teixidor. *Eur. J. Inorg. Chem.* **16**, 2385 (2010).
28. (a) W. M. Maxwell, V. R. Miller, R. N. Grimes. *Inorg. Chem.* **15**, 1343 (1976); (b) W. M. Maxwell, V. R. Miller, R. N. Grimes. *J. Am. Chem. Soc.* **96**, 7116 (1974).
29. X. Meng, S. Waterworth, M. Sabat, R. N. Grimes. *Inorg. Chem.* **32**, 3188 (1993).
30. We thank one of the referees for this suggestion.
31. X. Meng, S. Waterworth, M. Sabat, R. N. Grimes. *Inorg. Chem.* **32**, 3188 (1993).